



TEST OF A QUARK-DIQUARK FRAGMENTATION MECHANISM IN PROTON-PROTON
INTERACTIONS AT 360 GeV/c

EHS-RCBC Collaboration

Bombay¹-Budapest²-Genova³-CERN⁴-Chandigarh⁵-Innsbruck⁶-Japan (UG)⁷-Madrid⁸-
Mons⁹-Moscow¹⁰-Rutgers¹¹-Serpukhov¹²-Tennessee¹³-Vienna¹⁴ Collaboration

J.L. Bailly⁹, A. Batunin¹², B. Buschbeck¹⁴, C. Caso³, Y. Chiba^{7(a)},
H. Dibon¹⁴, F.J. Diez-Hedo⁸, T. Emura^{7(b)}, B. Epp⁶, A. Ferrando⁸,
F. Fontanelli³, T. Gémesy², P. Girtler⁶, I.V. Gorelov¹⁰, A. Gurtu¹,
R. Hamatsu^{7(c)}, Ph. Herquet⁹, T. Hirose^{7(c)}, J. Hrubec¹⁴, Y. Iga^{7(c)},
E. Kistenev¹², T. Kobayashi^{7(c)}, J.M. Kohli⁵, S. Krasznovszky²,
P.K. Malhotra¹, J.C. Marin⁴, M. Markytan¹⁴, I.S. Mittra⁵, L. Montanet⁴,
G. Neuhofer⁴, G. Pinter², P. Porth¹⁴, T. Rodrigo⁸, J.B. Singh⁴,
S. Squarcia³, K. Sudhakar¹, L.A. Tikhonova¹⁰, U. Trevisan³,
T. Tsurugai^{7(c)}, V. Yarba¹² and G. Zholobov¹²

- 1 Tata Institute of Fundamental Research, Bombay, India
- 2 Central Research Institute for Physics, Budapest, Hungary
- 3 University of Genova and INFN, Genova, Italy
- 4 CERN, European Organization for Nuclear Research, Geneva, Switzerland
- 5 Punjab University, Chandigarh, India
- 6 Inst. für Experimentalphysik, Innsbruck, Austria^(*)
- 7(a) Hiroshima University, Hiroshima, Japan
- (b) Tokyo University of Agriculture and Technology, Tokyo, Japan
- (c) Tokyo Metropolitan University, Tokyo, Japan
- (d) Chuo University, Tokyo, Japan
- 8 Junta de Energia Nuclear, Madrid, Spain
- 9 Université de l'Etat, Faculté des Sciences, Mons, Belgium
- 10 Moscow State University, Moscow, USSR
- 11 Rutgers University, New Brunswick, New Jersey, USA
- 12 Inst. for High Energy Physics, Serpukhov, USSR
- 13 University of Tennessee, Knoxville TN, USA
- 14 Inst. für Hochenergiephysik, Vienna, Austria^(*)

Submitted to Zeitschrift für Physik C

(*) Supported by Fonds zur Förderung der Wissensch. Forschung.

ABSTRACT

Feynman x distributions for the inclusive reactions $P + P \rightarrow \text{hadron} + \text{anything}$ at 360 GeV/c are analyzed in terms of a quark-diquark fragmentation model. The proton is assumed to be composed either of a quark and a diquark or of three independent quarks. The model tested includes a hadronization part for which we use the Field-Feynman and LUND fragmentation functions. The model with diquarks gives a better description of our experimental data; in particular for $P + P \rightarrow \Lambda^0 + \text{anything}$, the model without diquarks fails to reproduce the data.

1 INTRODUCTION

Precise measurements of the longitudinal momentum distributions in low p_T hadron-hadron collisions are available in the several hundred GeV energy region [1-7]. Using these data, one can study the reaction mechanisms of soft hadronic processes. Most models succeed in describing particular aspects of these processes, leaving others unexplained. It is thus quite challenging to construct a model which can achieve an overall description of low p_T multiparticle processes.

In this paper, we present a model based on a quark-diquark configuration and compare its predictions with the single particle distributions obtained in proton-proton collisions at 360 GeV/c [8,9,10].

Recently several experimental observations have brought some support to the diquark picture of the nucleon. For instance, the ABCDHW collaboration has observed a high production rate of protons with large p_T (3.5 - 4.4 GeV/c) at the ISR [11]. They have pointed out that a quark-diquark model could well reproduce the angular distributions of the protons, and that a model without diquarks gave a cross section far smaller than the observed one. Not only in large p_T hadron-hadron [12] and deep inelastic lepton-hadron collisions [13,14] but also in e^+e^- annihilations, one has obtained larger production cross sections of baryons [15,16] than expected from ordinary models in which no specific diquark systems are taken into account. Assuming 14% of a diquark system directly coupled to the virtual photon in e^+e^- annihilations [17,18], one could reach a good agreement with the data i.e. $e^+e^- \rightarrow \Lambda$.

As mentioned above, experimental data indicating the existence of a diquark system are mainly obtained in hard processes where the point-like treatment of a quark is allowed; thus perturbative QCD is applied to describe the scattering processes.

On the other hand, in soft processes, quarks or diquarks in a nucleon should be regarded as extended objects, so-called dressed valence quarks, in which effects of gluons and sea quarks are included. As illustrated in fig. 1, we assume for soft hadronic processes that one of the dressed

quarks (or diquarks) "i" is knocked out from the proton "a" and then hadronizes into hadron "c". A knowledge of the dressed quark (diquark) distributions in the nucleon "a" and their hadronization mechanisms is needed for this analysis.

For the hadronization mechanism, we have used both the Field-Feynman model (denoted FF) [19,20] and the Lund string model (LUND) [21,22]. Here the "LUND" model does not mean the full model to describe the complete process of hadron production in hadron-hadron collisions, but only the fundamental mechanism of producing hadrons through breaks of strings stretched between quarks or diquarks. Using various distributions from $e^+e^- \rightarrow$ hadrons obtained by the TASSO group [23], we could fix all the parameters introduced by these models. Then we studied the dressed quark (diquark) distributions in the nucleon using the parameterization provided by the Dual Regge framework. Here the diquark means an object which does not break into two quarks in the hadronization process. We assumed two types of distribution functions i.e., with or without a dressed diquark in the proton.

In order to predict single particle distributions, we combined in a Monte-Carlo program the distribution functions with the hadronization models (FF or LUND). In this analysis we concentrate on the longitudinal distribution of a single hadron (charged hadrons, π^0 , K_s^0 , Λ^0 , $\bar{\Lambda}^0$) in proton-proton collisions.

Data reduction is described in sect. 2. We derive the quark and diquark distribution functions in sect. 3 and try to fix the model (FF and LUND) parameters in sect. 4. Paying particular attention to the diquark system, we make a detailed comparison between the data and the model predictions in sect. 5. Sect. 6 presents a discussion of our results and our conclusions.

2 EXPERIMENTAL PROCEDURE AND DATA REDUCTION

The data used in this analysis were obtained from an experiment performed at CERN with the European Hybrid Spectrometer (EHS) including the 80 cm Rapid Cycling Bubble Chamber (RCBC) exposed to a beam of 360 GeV/c protons. A detailed description of the experimental set-up has been presented in ref. [8].

The inclusive π^0 distribution used in the present analysis has been discussed in a previous publication [9].

The bubble chamber pictures have been scanned and measured for inelastic interactions with at least one associated V^0 or γ seen in the bubble chamber. Detailed information on this analysis can be found in [10]. This sample corresponds to a sensitivity of 1.6 events/ μb . We selected events with good measurement quality by imposing that $\Delta p/p < 20\%$ where Δp and p are the error on the momentum measurement and the magnitude of this momentum, respectively, for charged particles. We treated all charged particles as π^\pm , except the slow protons identified by ionisation in RCBC. We have checked that the residual $\pi/\rho/K$ ambiguity does not affect the results in a significant way. It should be noted that the h^\pm distributions presented later correspond to single particle distributions for interactions associated with V^0 observed in the bubble chamber.

3 QUARK-DIQUARK DISTRIBUTIONS IN THE NUCLEON

According to the illustration given in fig. 1, the inclusive distribution of a hadron "c" coming from hadron "a" can be written as

$$\frac{1}{\sigma} \frac{d\sigma}{dx} = \sum_i \int_x^1 \frac{dx'}{x'} G_{a \rightarrow i}(x') D_{i \rightarrow c}\left(\frac{x}{x'}\right) \quad (1)$$

where the function $G_{a \rightarrow i}(x')$ denotes the dressed quark "i" distribution inside the hadron "a" and the function $D_{i \rightarrow c}(z)$ the fragmentation function of the dressed quark "i" to hadron "c". The x' denote the Feynman variable representing the fraction of longitudinal momentum of the parent hadron "a" carried by the quark "i", the quantity $z = x/x'$ stands for the same relation between the quark "i" and the produced hadron "c". In the following, we use the term "quark" when it is really meant a "dressed quark".

We now construct the quark distribution function $G_{a \rightarrow i}(x')$ based on the following two view-points [24,25,26]: (1) quarks in a nucleon form a diquark cluster so that a nucleon consists of a quark and a diquark (the quark-diquark configuration (denoted as QD)) and (2) three quarks are independent and thus no diquark system exists (denoted as IQ). Furthermore

we assume that the diquark cluster does not split into two quarks during hadronization. We may thus parametrize the momentum sharing function for the quark (or the diquark) in a nucleon based on these two view points as

$$h_{QD}^{(1)} \propto x^{\alpha_q} y^{\alpha_{qq}} \delta(1-x-y) \quad (2)$$

$$h_{IQ}^{(2)} \propto (xyz)^{\alpha_q} \delta(1-x-y-z) \quad (3)$$

where α_q and α_{qq} denote dynamical parameters and $x(y)$ corresponds to the momentum fraction of the quarks (diquarks). Using the relations (2) and (3), we write the quark distribution functions as

$$\begin{aligned} G_{QD}^{(1)}(x) &= \frac{1}{B(\alpha_q + 1, \alpha_{qq} + 1)} \int_0^1 dy h_{QD}^{(1)}(x,y) \\ &= \frac{1}{B(\alpha_q + 1, \alpha_{qq} + 1)} x^{\alpha_q} (1-x)^{\alpha_{qq}} \end{aligned} \quad (4)$$

$$\begin{aligned} G_{IQ}^{(2)}(x) &= \frac{1}{B(\alpha_q + 1, 2\alpha_q + 2)} \int_0^1 dy dz h_{IQ}^{(2)}(x,y,z) \\ &= \frac{1}{B(\alpha_q + 1, 2\alpha_q + 2)} x^{\alpha_q} (1-x)^{2\alpha_q + 1} \end{aligned} \quad (5)$$

where $B(x, y)$ denotes the beta function. As Kinoshita et al. [26] proposed, we can regard the parameters $-\alpha_q$ and $-\alpha_{qq}$ as the intercepts of Regge trajectories of mesons and baryoniums, respectively. From the ρ - ω trajectory, we have $\alpha_q = -1/2$ for u and d quarks. In order to determine α_{qq} , we need knowledge of baryonium trajectories for which we have no reliable experimental information. However, there are some theoretical suggestions [27,28] that $0.5 < \alpha_{qq} < 2$. We show in fig. 2 the x dependence of the distribution functions (4) for $\alpha_{qq} = 0.5, 1.0, 2.0$ (solid lines) together with the distribution function (5) (dashed line). The essential difference between these two distribution functions is that the quark-diquark configuration attributes to the quark smaller momenta, thus leading to higher momenta of the diquark than those given by the independent quark system. This can also be seen in the average values of x for the quark and diquark in a proton. In the case of three independent quarks, the quark and the remaining two quarks have $\langle x \rangle = 1/3$ and $2/3$, respectively. The quark-diquark configuration gives rise to more extreme values as seen in table 1.

For the quark-diquark configuration, a proton state may be described as

$$|\text{proton}\rangle = \sqrt{A} |u, (ud)^A\rangle + \sqrt{S} \left(\frac{1}{\sqrt{3}} |u, (ud)^S\rangle - \sqrt{\frac{2}{3}} |d, (uu)\rangle \right) \quad (6)$$

where $(ud)^A$ and $(ud)^S$ indicate the antisymmetric and symmetric diquark states [26]. Here we shall assume the SU(6) limit where the antisymmetric state and the symmetric state are equally mixed, namely $A = S = 1/2$.

A more sophisticated treatment for the quark-diquark distribution functions might lead to a small modification of the single particle distributions [29,30]. However, the formulation presented here contains the essential properties of the dual Regge theory and thus should be sufficient to describe single particle distributions.

4. MODELS FOR HADRONIZATION

To describe the hadronization process, we have used the Monte-Carlo program EPOCS [31] developed for the reaction $e^+e^- \rightarrow \text{hadrons}$. EPOCS consists of two parts corresponding to the elementary process $e^+e^- \rightarrow q\bar{q}, q\bar{q}g$ where q and g denote quarks and gluons respectively and the hadronization process formulated by the FF or LUND models.

Using the data of $e^+e^- \rightarrow \text{hadrons}$ at $\sqrt{s} = 34$ GeV obtained by the TASSO group [23], we have determined the parameters in the FF and LUND models as shown in table 2. Both models have the following parameters in common; (a) the QCD scale parameter Λ ; (b) the production rate of vector to pseudoscalar mesons V/PS (or similarly decuplet to octet baryons); (c) the suppression factor of a strange quark η_s , (d) the intrinsic transverse momentum k_T of the quark with respect to the direction of the parent quark, and (e) the diquark pick up rate from the sea ξ_d . There are still a few parameters specific to each model. The fragmentation function $f(z)$ takes the following form

$$f(z) = 1 - a_F + 3a_F(1-z)^2 \quad \text{for FF}$$

and

$$= (1 + c)(1-z)^2 \quad \text{for LUND,}$$

where the parameter z denotes the fraction of longitudinal momenta carried by a hadron. The parameter a_F in FF was also determined by comparing the model predictions with the TASSO data while we used the original Lund value of the parameter $c = 0.5$. The Sterman-Weinberg's two jet parameters ϵ , δ for FF and the parameter a_t (transverse mass) for LUND were fixed at the values proposed in the original work.

In order to find reasonable values for each parameter, we have extensively examined the consistency between the model predictions and various data provided by TASSO. We did not carry out a χ^2 fit but checked in detail how well we can reproduce various experimental distributions i.e. multiplicity of charged hadrons, thrust, sphericity, transverse momentum and so on. We also checked the energy dependence of the parameters for the TASSO data between 14 and 34 GeV. A detailed description of this adjustment will be published elsewhere.

The transverse momentum of hadrons have been generated according to the Gaussian function $\exp(-p_T^2/2\langle k_T^2 \rangle)$.

5. MODEL PREDICTIONS AND EXPERIMENTAL RESULTS

We now turn to a description of small p_T hadronic processes, i.e. $pp \rightarrow \text{hadron} + X$ and compare the model predictions to our experimental results.

The quark-diquark distribution function (4) is combined with the hadronization distributions given by the Field-Feynman or the Lund models, and this procedure is repeated for the independent quark distribution function (5). The method ensures the conservation of all quantum numbers which must be preserved in the overall process.

Since we find no significant differences, at this level of the analysis, between the results obtained using the Field-Feynman or the Lund Models, we choose to illustrate our results in the following by comparing the experimental data to the predictions obtained with Field-Feynman.

We generated events by EPOCS with or without diquarks taking into account the fact that the experimental data contains only events with associated V^0 . This property of the events led to very small effects as shown in fig. 3 for inclusive charged hadron distribution.

Figs 4(a)-4(f) show the single particle distributions together with the model predictions in which the distribution functions (4) with $\alpha_{qq} = 1.0$ and (5) with $\alpha_q = -0.5$ are combined with the FF fragmentation function. Using $\alpha_{qq} = 0.5, 2.0$, we found no significant difference in the single particle distributions (not shown). It should be noted that the overall normalization of the model is made only to the inclusive cross section for negative hadron production as obtained in [9] but the model can predict relative production rates for $h^+, K_S^0, \Lambda^0, \Lambda^0$ which agree well with the data as shown in table 3. However, h^+ consists of not only non diffractive production, but also diffraction dissociation which our model cannot predict. If we assume that the difference between the data and the model prediction beyond $|X_F| = 0.65$ is due to diffraction dissociation, we find that the diffractive cross section for $PP \rightarrow h^+ + \text{anything}$ at 360 GeV/c is $\$.6$ mb which is in reasonable agreement with other experiments, considering that we have not introduced the corrections for trigger losses.

With the exception of the region $|X_F| > 0.65$ for the $PP \rightarrow h^+ + X$ distribution, there is in general excellent agreement between the predictions using the quark-diquark configuration and the data.

The diquark system (ud) with spin 0, which is the largest component in the proton wave function (see eq. (6)), is the dominant contribution to Λ^0 production, so that the large diquark fraction with high momentum plays an essential role in Λ^0 production in the large X_F region, i.e. $|X_F| > 0.3$. A similar but less significant effect is also seen in the h^+ distribution (fig. 4(b)) where the quark-diquark configuration gives rise to a higher cross section for $|X_F| > 0.3$ than the independent quark systems. This is due to the contribution of protons in h^+ being distributed widely over the whole X_F region. The independent quark model does not give a good interpretation of the data; the disagreement is particularly striking for the Λ distribution.

To estimate the influence of the quark and diquark structure functions used in this analysis, we have repeated the calculations, setting $G(x')$ equal to 1 in eq. (1) but keeping the hadronization unchanged: the results are shown by the dotted curves in figs 4(a) to 4(f). As expected, these curves show softer x distributions than those obtained with the diquark structure function and underline, in particular for the Λ distribution, the need of a non trivial diquark structure function.

6. DISCUSSION AND CONCLUSIONS

We have successfully constructed a model which can quantitatively describe various kinds of data for $e^+e^- \rightarrow$ hadrons and $PP \rightarrow$ hadrons. The essential ingredients of this model are: the quark-diquark distribution in the proton and the hadronization mechanism for quarks or diquarks.

Using the Monte-Carlo program EPOCS, we have studied the three different possibilities obtained by combining the distribution function of an independent quark system with the FF model and that of a quark-diquark configuration with the FF or LUND model. Comparing the model predictions with $PP \rightarrow h^\pm, \pi^0, K_S^0, \Lambda^0, \bar{\Lambda}^0$ at 360 GeV/c, we found that the diquark plays an essential role which was most clearly exhibited in the Λ^0 distribution. The diquark in our model is regarded as a single entity ($\bar{3}$ of colour) which will reappear as a constituent of the produced baryons. U.P. Sukhatme et al. [32] proposed a more detailed treatment of the diquark system in the proton which does not seem to be necessary here.

Finally, we would like to mention the extensive study of diquarks by S. Fredriksson et al. [33,34,35]. They have revealed several interesting aspects of the diquark emerging from hard processes. According to their arguments, the proton dominantly consists of a u quark and a (ud) diquark with spin 0 and the size of the diquark is about 0.2 fm. Consequently, the diquark can couple directly to a virtual photon in e^+e^- giving rise to significant effects for the R -ratio in the charmonium region [18] the (uc) diquark having large coupling to the charge $4/3$. If these features are taken into account, one should be able to extend the present work to other features of our experimental data [36].

6. ACKNOWLEDGEMENTS

We are indebted to the CERN staff, whose sterling performance was essential in collecting the data for this experiment. We also would like to take the opportunity to acknowledge the heroic effort by our scan and measurement personnel in the participating labs and Miss M. King for invaluable assistance in typing this paper.

REFERENCES

- [1] H. Kichimi et al., Phys. Rev. D20 (1979) 37.
- [2] S. Erhan et al., Phys. Lett. 85B (1979) 447.
- [3] A. Sheng et al., Phys. Rev. D11 (1979) 1733.
- [4] A. Suzuki et al., Phys. Rev. D24 (1981) 605.
- [5] T. Kafka et al., Phys. Rev. D16 (1979) 1261.
- [6] A. Gurtu et al., Zeitsch. für Phys. C21 (1984) 143.
- [7] A.E. Brenner et al., Phys. Rev. D26 (1984) 1497.
- [8] J.L. Bailly et al., Zeitsch. für Phys. C23 (1984) 205.
- [9] J.L. Bailly et al., Zeitsch. für Phys. C22 (1984) 119.
- [10] M. Asai et al., Zeitsch. für Phys. C27 (1985) 11.
- [11] A. Breakstone et al., Zeitsch. für Physik C28 (1985) p. 335.
- [12] H. Frisch et al., Phys. Rev. D27 (1983) 1001.
- [13] M. Arneodo et al., CERN/EP 84-71, 20 June 1984.
- [14] C.C. Chang et al., Phys. Rev. D27 (1983) 2776.
- [15] R. Brandelik et al., Phys. Lett. 105B (1981) 75.
- [16] W. Bartl et al., Phys. Lett. 104B (1981) 325.
- [17] T. Mayer, DESY 81-046, August 1981.
- [18] S. Ekelin, S. Fredriksson, M. Jandel and T.I. Larsson, Phys. Rev. D28 (1983) 257.
- [19] R.D. Field, R.P. Feynman and G.G. Fox, Nucl. Phys. B128 (1977) 1.
- [20] R.D. Field and R.P. Feynman, Phys. Rev. D15 (1977) 2590;
R.D. Field and R.P. Feynman, Nucl. Phys. B136 (1978) 1.
- [21] B. Andersson, G. Gustafson and B. Soderberg, Zeitsch. für Phys. C20 (1983) 317.
- [22] T. Sjostrand, Computer Phys. Comm. 28 (1983) 229.
- [23] M. Althoff et al., Zeitsch. für Phys. C22 (1984) 307.
- [24] A. Capella et al., Phys. Lett. 81B (1979) 68;
A. Capella, U. Sukhatme and J. Tran Than Van, Zeitsch. für Phys. C3 (1980) 329;
G. Cohen-Tannoudji et al., Phys. Rev. D19 (1979) 3397.

REFERENCES (Cont'd)

- [25] H. Minakata, Phys. Rev. D20 (1979) 1656.
- [26] K. Kinoshita et al., Zeitsch. für Phys. C4 (1980) 103;
K. Kinoshita, H. Noda and T. Tashiro, Prog. Theor. Phys. 68 (1982)
1699, 2086.
- [27] M. Uehara, Prog. Theor. Phys. 59 (1978) 1587.
- [28] T. Inami, K. Kawarabayashi and S. Kitakado, Phys. Rev. D19 (1979) 129.
- [29] A.V. Batunin, A.K. Likhoded and A.N. Tolstenkov, Serpukhov Preprint
(1984) 131.
- [30] V.V. Anisovich, M.N. Kobrinsky and J. Nyiri, Leningrad Preprint
(1984) 982.
- [31] K. Kato and T. Munehisa, KEK Report 84-18, e^+e^- event generator EPOCS
(in Japanese).
- [32] U.P. Sukhatme, K.E. Lassila and R. Orava, Phys. Rev. D25 (1982) 2975.
- [33] S. Fredriksson, M. Jandel and T. Larsson, Zeitsch. für Phys. C19
(1983) 53.
- [34] S. Fredriksson, Phys. Rev. Lett. 50 (1984) 724.
- [35] S. Fredriksson, 19th Rencontre de Moriond, Vol. 2 (1984) 479.
- [36] T. Tsurugai et al., EHS-RCBC Collaboration, work in progress.

TABLE 1

Average momentum fraction $\langle x \rangle$ of a quark and a diquark (two-quark) both for the three quarks (IQ) and quark-diquark (QD) configurations

		$\langle x \rangle$	
		quark	two quarks
IQ	$\alpha_q = -0.5$.33	.67
QD	α_{qq}		
	0.5	0.28	0.72
	1.0	0.22	0.78
	2.0	0.17	0.83

TABLE 2

Values of parameters used in the Field-Feynman and LUND models. Details of each parameter are described in the text.

FF	LUND
Λ (GeV) = 0.4	0.4
V/PS = 1	1
$\eta_s = 0.3$	0.3
$\langle k_T \rangle$ (GeV/c) = 0.42	0.38
$\xi_d = 0.03$	0.03
$a_F = 0.57$	$c = 0.5$
$\epsilon = 0.1$	$a_t = 1$ GeV
$\delta = 0.1$	

TABLE 3

Experimental results and model predictions for inclusive cross sections

	Experiment (mb)	Model prediction (mb)
h^-	116 ± 5	116
h^+	181 ± 2	170
π^0	132 ± 11	141
K_s^0	8.55 ± 0.51	8.28
Λ^0	4.08 ± 0.40	5.00
$\bar{\Lambda}^0$	0.43 ± 0.12	0.31

FIGURE CAPTIONS

- Fig. 1 Parton diagram of quark and diquark hadronization.
- Fig. 2 X dependence of the distribution functions predicted from the three quark configuration (dotted line) and the quark-diquark configuration with $\alpha_{qq} = 0.5, 1.0, 2.0$ (solid line).
- Fig. 3 The Monte-Carlo predictions from the quark-diquark configuration combined with the Field-Feynman model for events with or without v^0 .
- Fig. 4 Comparison of the model predictions with data. Solid line; the quark-diquark configuration combined with the FF model. Dashed line; the three independent quarks combined with the FF model. Dotted line: the FF predictions, setting $G(x') = 1$ in eq. (1).

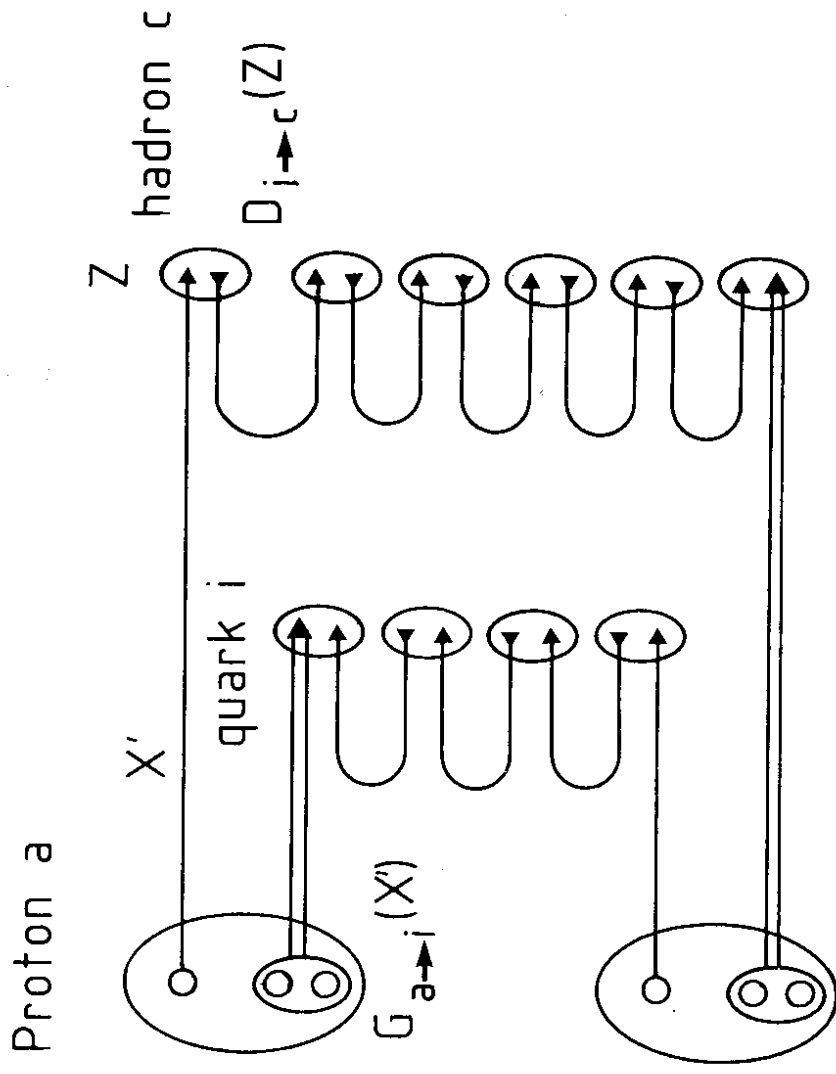


Fig.1

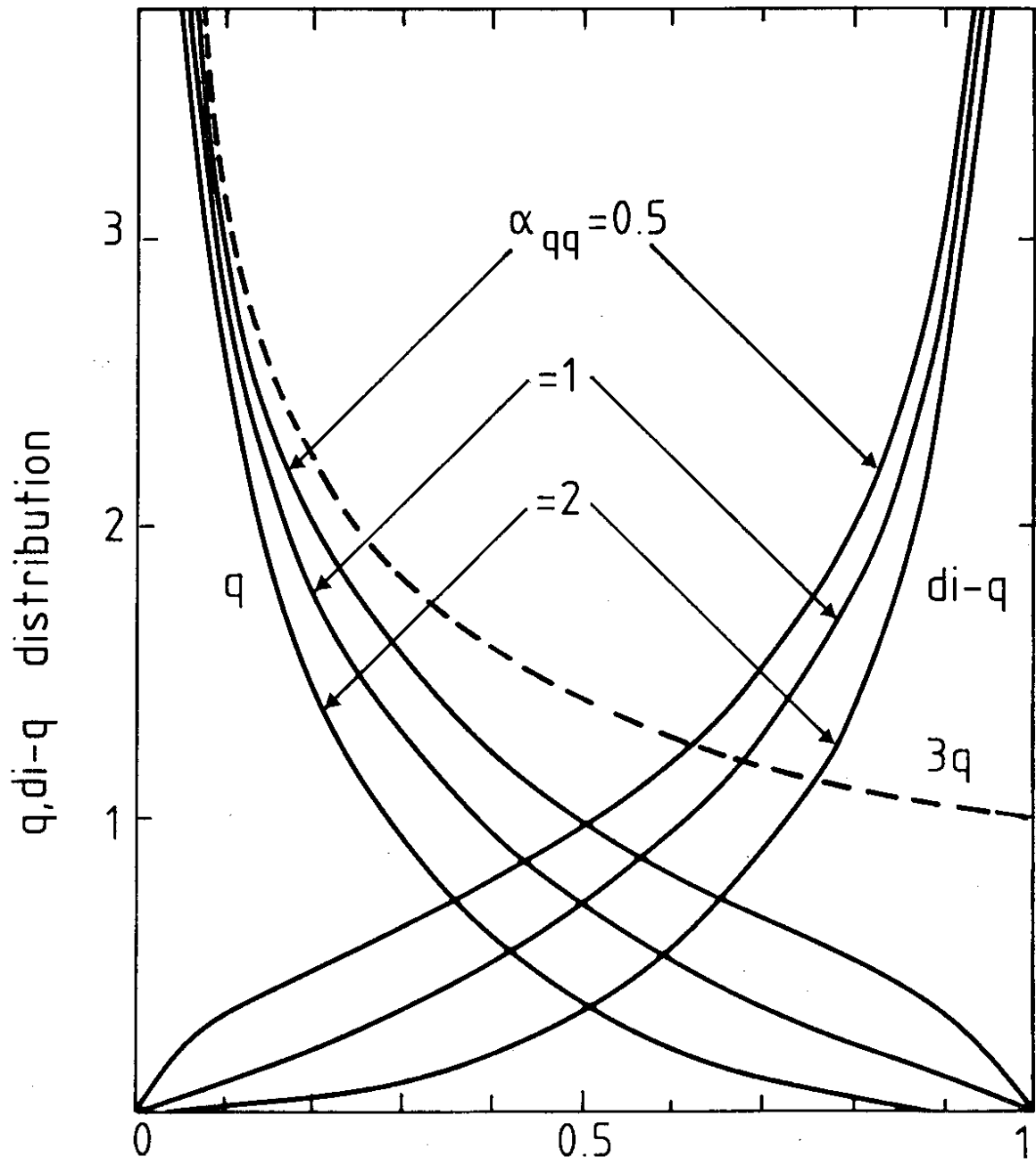


FIG. 2

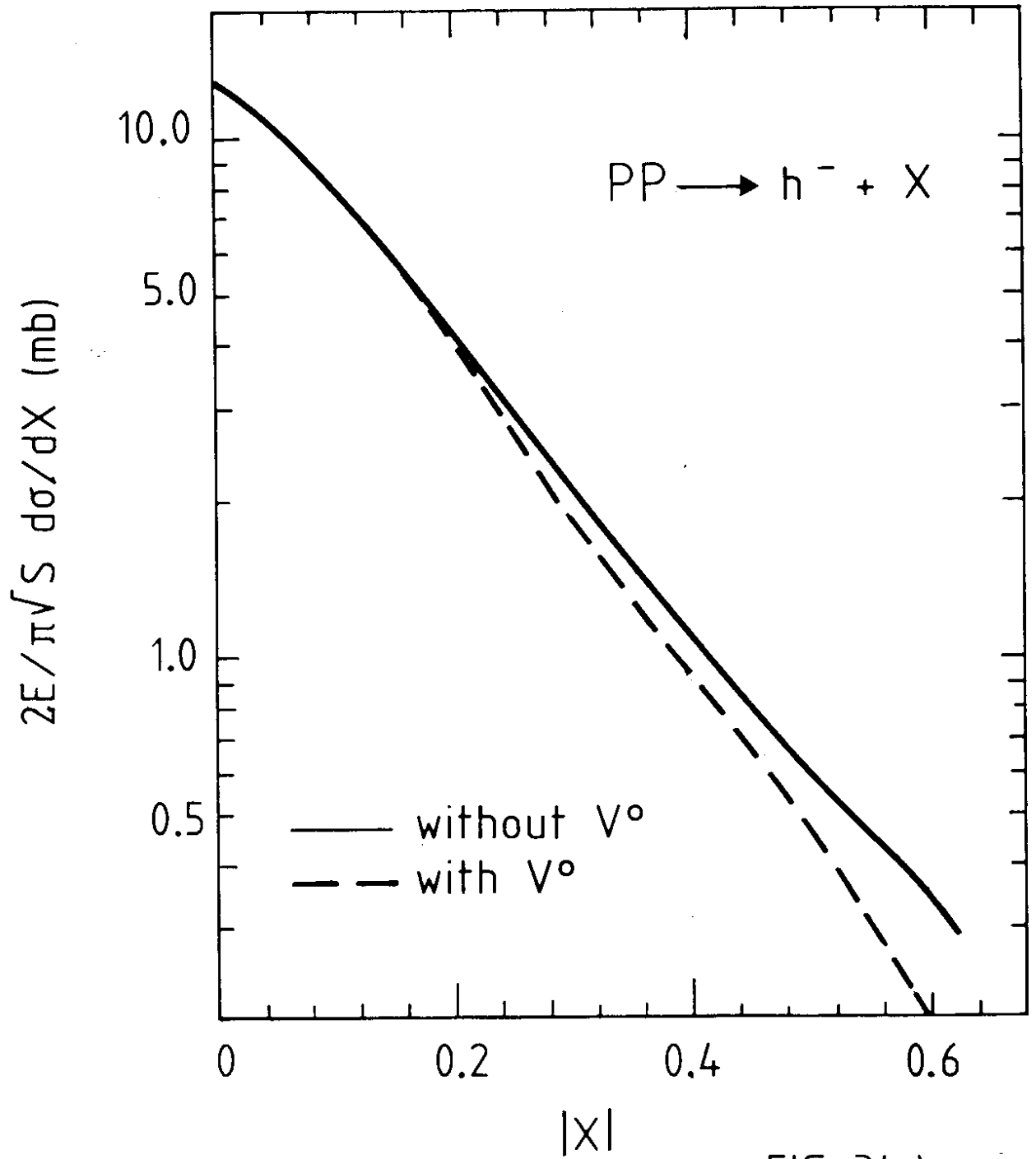


FIG. 3(a)

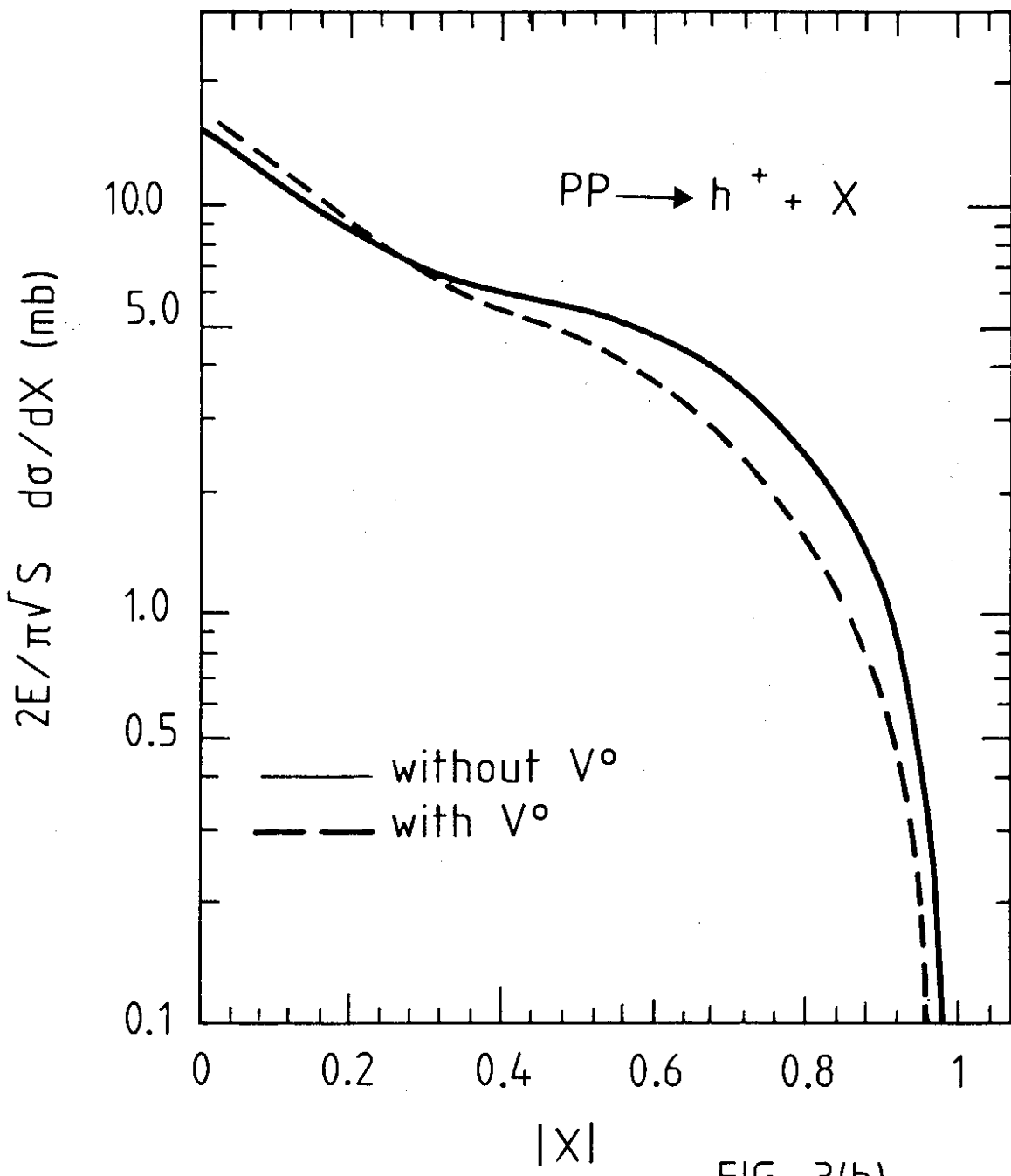


FIG. 3(b)

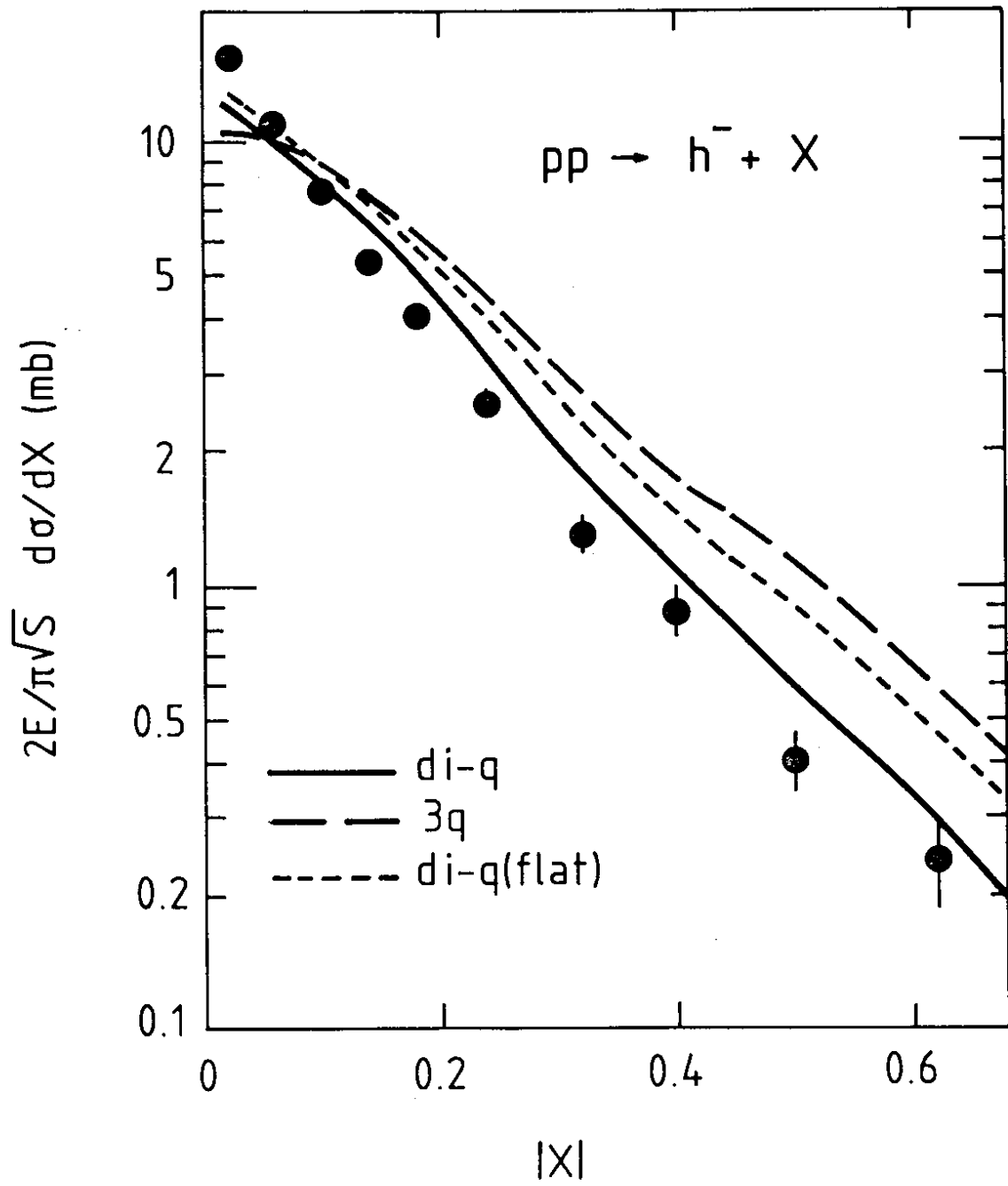


FIG. 4a

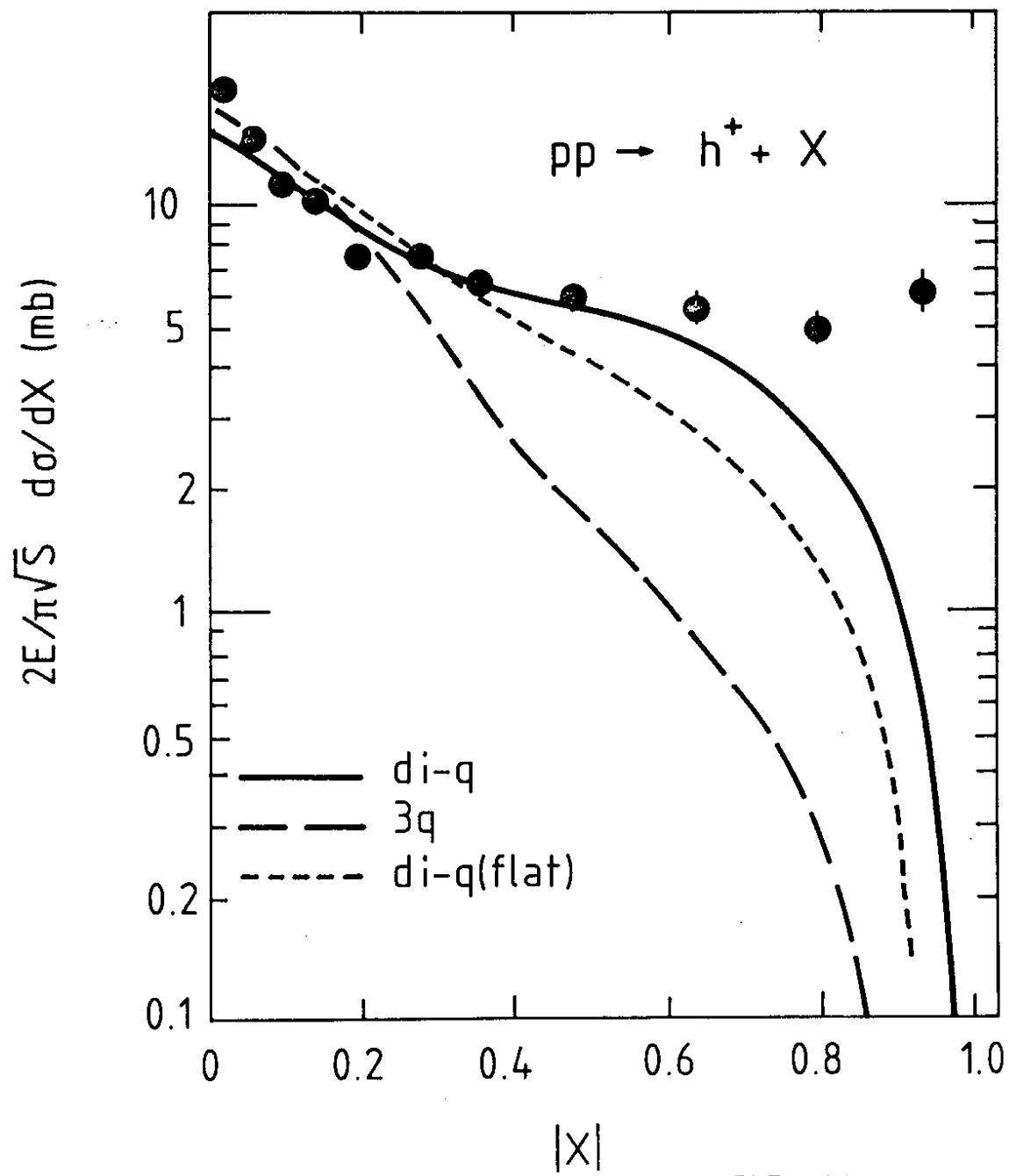


FIG. 4b

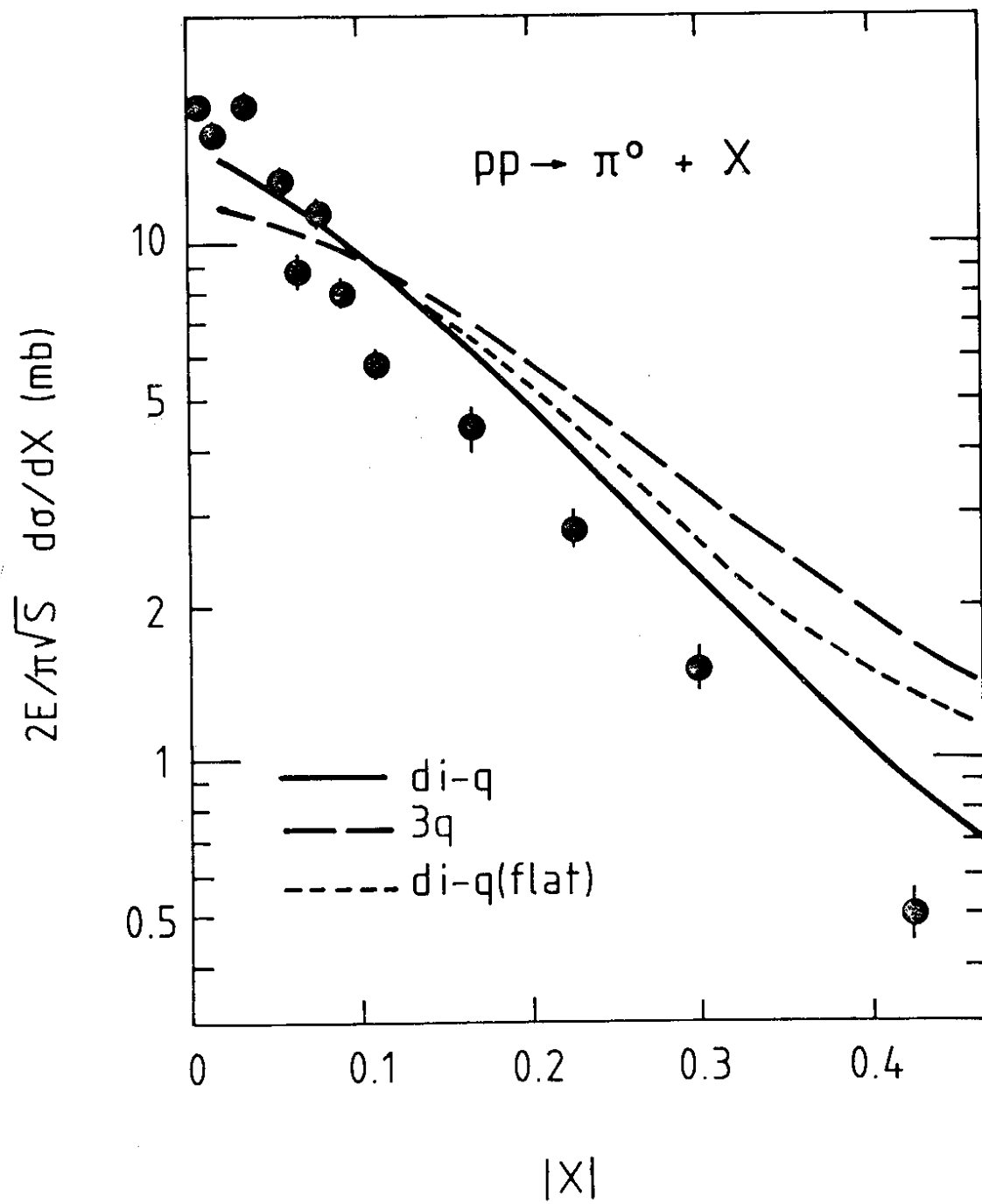


FIG. 4c

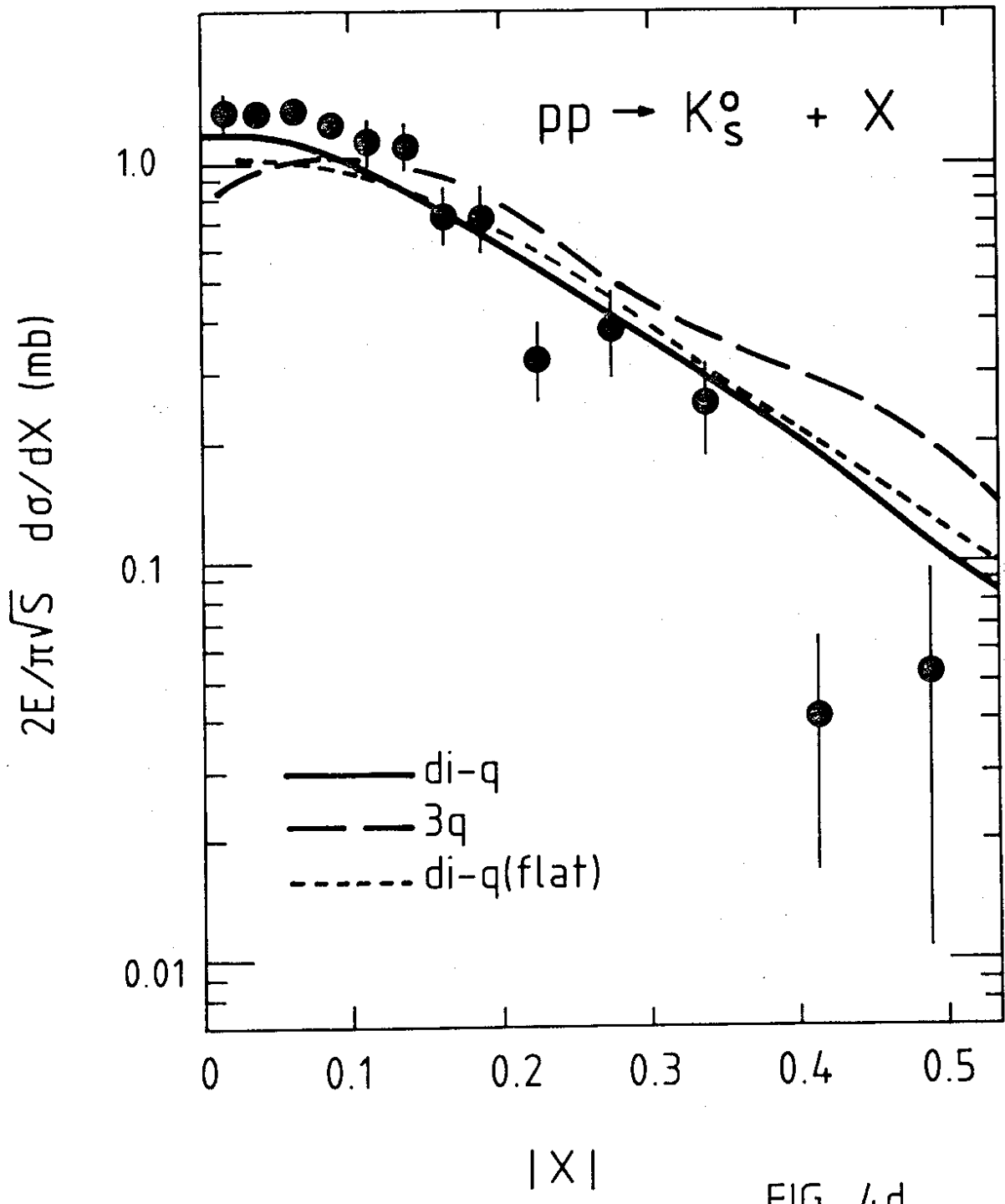


FIG. 4d

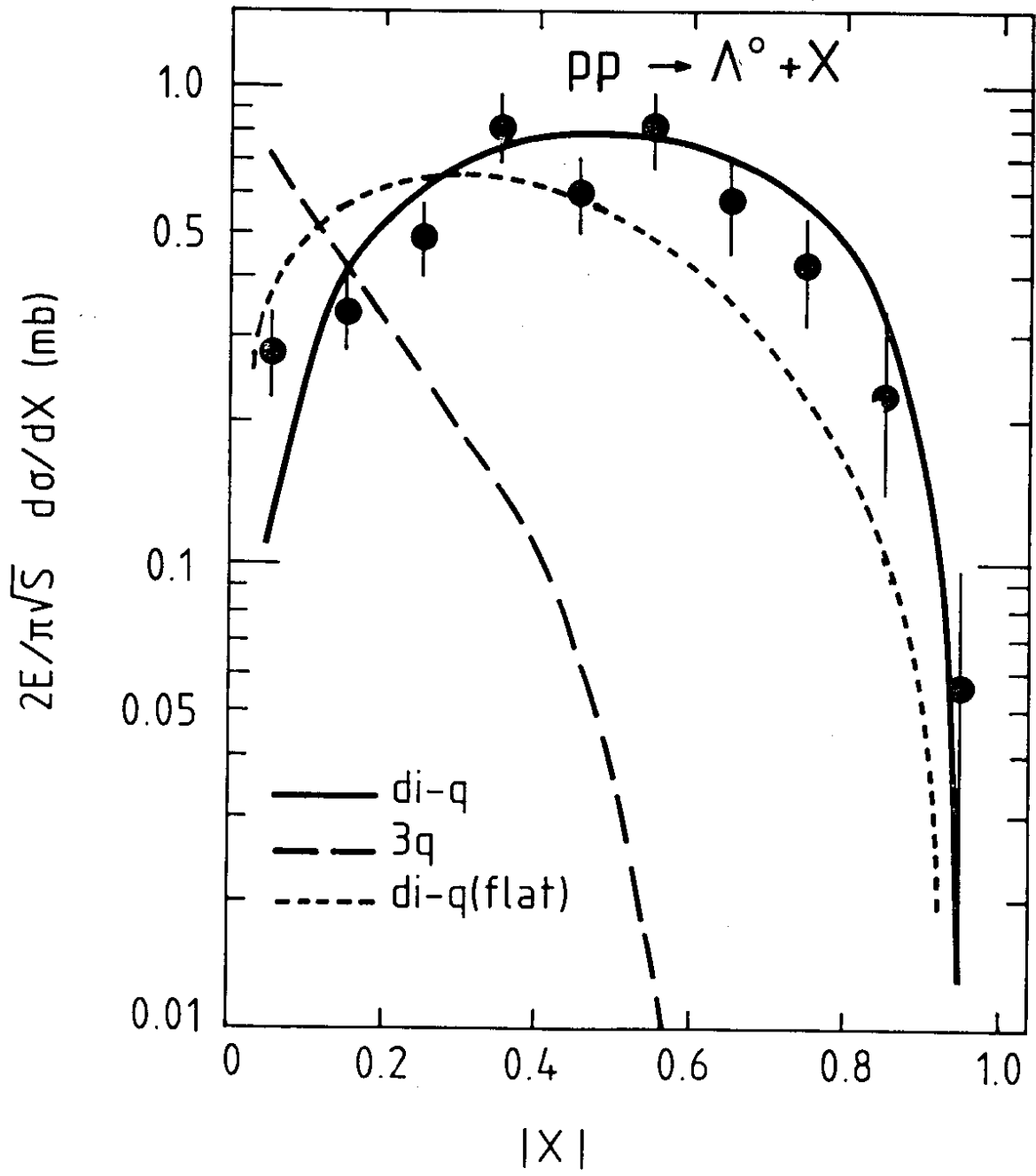


FIG. 4e

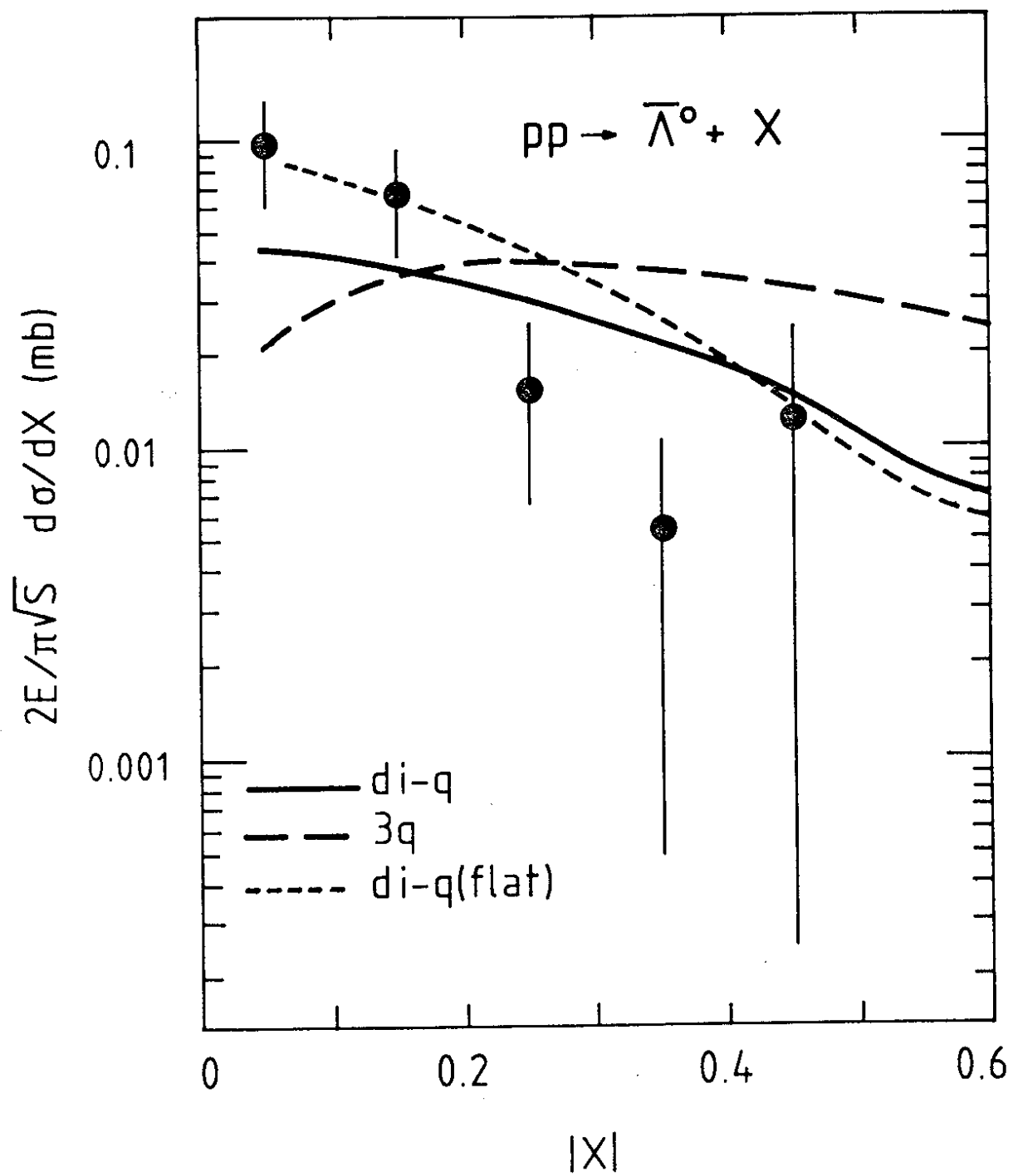


FIG. 4f